

Trace Elements Characteristics of Black Shales from the Ediacaran Doushantuo Formation, Hubei Province, South China: Implications for Redox and Open vs Restricted Basin Conditions

Bi Zhu^{1,3}, Shaoyong Jiang^{2,3*}, Daohui Pi², Lu Ge¹, Jinghong Yang³

1. Institute of Isotope Hydrology, School of Earth Sciences and Engineering, Hohai University, Nanjing 210098, China
2. State Key Laboratory of Geological Processes and Mineral Resources, Faculty of Earth Resources, Collaborative Innovation Center for Exploration of Strategic Mineral Resources, China University of Geosciences, Wuhan 430074, China
3. State Key Laboratory for Mineral Deposits Research, School of Earth Sciences and Engineering, Nanjing University, Nanjing 210093, China

ABSTRACT: In the present study, we carried out trace element analyses of black shales of the Ediacaran Doushantuo Formation from two sections (Jiulongwan, Baiguoyuan) in Hubei Province, South China. Mo-U characteristics of black shales from the two sections and compiled Mo-U data of Doushantuo black shales from sections of a variety of sedimentary facies described the temporal/spatial variability in the redox conditions of paleo-seawater during deposition of the Doushantuo Formation. Changes in Mo-U patterns of the Doushantuo Member II (DST2) shales of open marine environments are consistent with a shift from a predominately oxic to a predominately anoxic ocean during their deposition. Mo-U patterns of the DST2 black shales from intra-shelf sections reflect basin restriction may have happened in the intra-shelf basin and are compatible with the redox-stratified model of the intra-shelf basin. Mo-U patterns of black shales of the Doushantuo Member IV (DST4) reveal that the shales from intra-shelf sections have more pronounced Mo enrichment and more significant enrichment of Mo over U than the slope shales, indicating the operation of a Mn particulate shuttle in the intra-shelf basin. High Mo/TOC ratios of the DST4 at the intra-shelf sections, in combination with similar Mo-TOC patterns of the DST4 from both intra-shelf and slope sections, indicate the intra-shelf basin was well connected to the open ocean during deposition of the DST4.

KEY WORDS: Doushantuo Formation, Mo-U covariation, Mo/TOC, south China

0 INTRODUCTION

The Neoproterozoic Ediacaran period encompasses a unique interval of Earth history between the termination of the global Marinoan glaciation (~635 Ma) and the beginning of Cambrian biological radiation (Condon et al., 2005; Knoll et al., 2004). This distinctive time period is characterized by major changes in the evolution of life such as radiation of complex multicellular life (Xiao et al., 2014; McCall, 2006; Brasier and Antcliffe, 2004; Xiao et al., 1998). Moreover, this unique time period is also marked by dramatic changes in the atmospheric–oceanic system such as oxygenation of the deep ocean (Li et al., 2016; Lyons et al., 2014; Sahoo et al., 2012; McFadden et al., 2008; Canfield et al., 2007; Fike et al., 2006), and substantial fluctuations in concentrations and isotopic compositions of elements (e.g. carbon, sulfur, strontium, moly-

Manuscript accepted February 7, 2017.

bdenum) in seawater (Chen et al., 2015; Bjerrum and Canfield, 2011; Halverson et al., 2010; Kendall et al., 2009; Ries et al., 2009; McFadden et al., 2008; Halverson et al., 2007; Fike et al., 2006; Knoll et al., 2006).

The Ediacaran successions in South China cover a wide range of sedimentary facies from continental shelf to deep basin with comparatively good records of rocks and fossils (Zhu et al., 2007; Zhu et al., 2003). The Ediacaran strata in the Three Gorges area in Hubei Province is the type locality for the late Neoproterozoic (i.e. Ediacaran) system. These Ediacaran successions have been intensively investigated over the past decades, which has greatly advanced the understanding of the evolution of multicellular life, the atmospheric–oceanic system and the local palaeogeographical conditions during the Ediacaran period. Recent studies have demonstrated that the paleogeographic settings and depositional environments during this important Earth interval on the Yangtze platform may have been more complex than previously thought (Och et al., 2015; Zhu M et al., 2013; Jiang et al., 2011; Vernhet and Reijmer,

*Corresponding author: shyjiang@cug.edu.cn

© China University of Geosciences and Springer-Verlag Berlin Heidelberg 2017

Manuscript received October 6, 2016.

2010). Consequently, the complexity in palaeo-topography would introduce additional complexity like basin restriction and more complicated spatial variability in the redox conditions of paleo-seawater across this region.

Redox-sensitive elements like U, Mo, Ni, etc. have long been used as sensitive indicators for redox conditions of depositional environments in the oceans (Tribovillard et al., 2006). Recent studies of marine sediments have identified a range of new applications using trace-metal data like Mo/U and Mo/TOC ratios in the analysis of palaeoceanographic system (Algeo and Rowe, 2012; Tribovillard et al., 2012; Algeo and Tribovillard, 2009; Algeo and Lyons, 2006). In this study, trace elements and TOC data for black shales of the Doushantuo Formation from two sections (Jiulongwan, Baiguoyuan) in Hubei Province, combined with previously published Mo-U, TOC and Fe speciation data of Doushantuo shales from other sections of different sedimentary facies (intra-shelf, upper and lower slope, basin), were used to investigate the temporal/spatial variations in redox conditions of seawater during this critical period and to evaluate possible basin restriction during deposition of these shales on the Yangtze platform.

1 GEOLOGICAL BACKGROUND AND SAMPLES

Ediacaran sedimentary successions are well exposed in the southeastern Yangtze block of South China, including the Doushantuo Formation (635–551 Ma) of mixed carbonate and siliciclastic rocks and the carbonates dominating Dengying Formation (551–542 Ma). Lack of major tectonic events and igneous activities during the deposition of the Doushantuo strata, and the analysis of patterns of thickness and distribution of the strata support a passive margin setting for its deposition (Jiang et al., 2011). The sedimentary facies and depositional environments for the Ediacaran strata in South China cover a variety of types from continental shelf to deep basin (Li et al., 2016; Jiang et al., 2011, Zhu et al., 2007, Zhu et al., 2003). It is also inferred that there was a transition in paleographic settings from open shelf to rimmed shelf lagoon during the deposition of the Ediacaran sedimentary successions soon after the Marinoan glaciation (Jiang et al., 2011). Thus the majority of the Doushantuo Formation in the Yangtze platform was deposited on a rimmed carbonate shelf with a barrier separated the shelf

lagoon from the open ocean (Fig. 1, Zhu M et al., 2013; Jiang et al., 2011; Vernhet and Reijmer, 2010). The two studied sections (Jiulongwan and Baiguoyuan) are located in the Three Gorges area in Hubei Province (Fig.1). According to paleogeographic reconstruction studies, the Doushantuo Formation at Jiulongwan and Baiguoyuan were deposited within the shelf lagoon, with the water depth deeper for the Jiulongwan section (Zhu M et al., 2013; Jiang et al., 2011).

The Doushantuo Formation in the Three Gorges area rests on the Marinoan-age Nantuo diamictite (Condon et al., 2005) and is overlaid by carbonates of the Ediacaran Dengying Formation. Generally, the Doushantuo Formation can be divided into four lithostratigraphic members in ascending order (Zhu et al., 2007): Member I (cap dolostone), Member II (alternating shale and dolostone), Member III (dolostone- and limestone-dominated), Member IV (carbonaceous black shale). Abundant fossils have been reported from the Doushantuo Formation in this area, with micro-fossils including acanthomorphic acritarchs, putative animal eggs and embryos, multicellular algae, and filamentous and coccoidal cyanobacteria for the Member II and III (Liu et al., 2014, 2013; McFadden et al., 2008; Yin et al., 2007; Zhou et al., 2007) and carbonaceous compressions of likely macroalgae for the Member IV (Xiao et al., 2002). Two precise zircon U-Pb ages for the interbedded volcanic tuff layers have constrained the Doushantuo Formation from 635 Ma to 551 Ma (Condon et al., 2005). Other dates for the Doushantuo Formation near this region include zircon U-Pb age of 614.0 ± 7.6 Ma reported from a volcanic tuff layer below an erosional unconformity (correlated with the middle part of Member II by Zhu et al. (2007) at the Wangjiagou section ~ 50 km NE of the Three Gorges area (Liu et al., 2009), and Re-Os ages of 543 ± 24 Ma and 591 ± 5 Ma for the Member IV black shales (Zhu B et al., 2013; Kendall et al., 2009). The stratigraphy and the sedimentary structure of the Jiulongwan and Baiguoyuan sections have been described in detail in Mi et al. (2010) and McFadden et al. (2008) and are shown in Fig. 2. At Jiulongwan, 29 black shale samples of the Member IV were collected from the base to the top. At Baiguoyuan, 7 black shale samples were collected above the phosphate-rich unit of the Member II (Table 1).

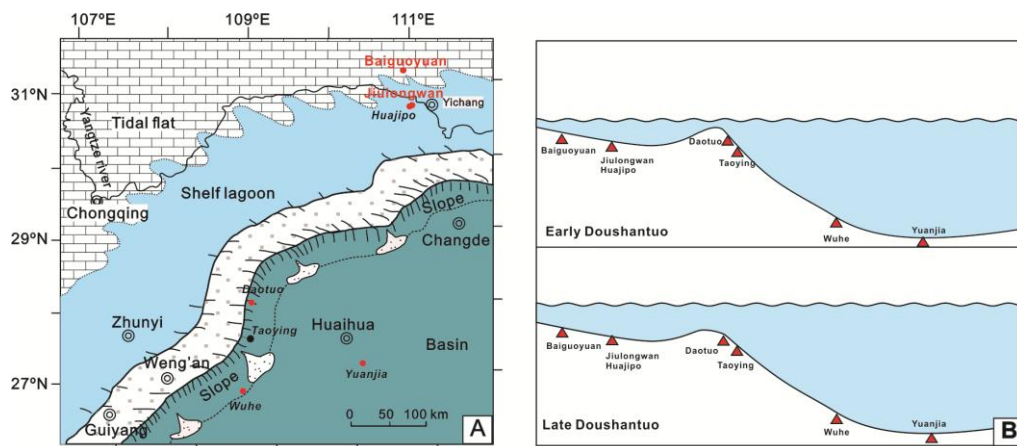


Figure 1 A: Depositional environment of the Doushantuo Formation. The two studied sections (Jiulongwan and Baiguoyuan) and other concerned sections (Wuhe, Taoying, Yuanjia, Daotuo) are indicated (Jiang et al., 2011); B: Palaeogeographic locations of the studied sections on the Ediacaran Yangtze platform. (Modified after Zhu M et al. 2013 and Jiang et al., 2011).

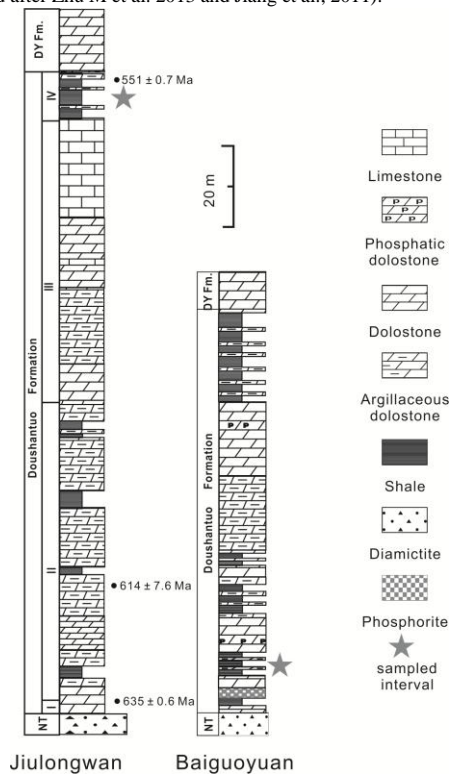


Figure 2 Simplified stratigraphic columns of the Doushantuo Formation at Jiulongwan and Baiguoyuan (after McFadden et al., 2008; Mi et al., 2010)

2 ANALYTICAL METHOD

All analyses were performed at the State Key Laboratory for Mineral Deposits Research of Nanjing University. For trace element analyses, the pre-treatment of the organic-rich samples followed the method of Scott et al. (2008). About 1 g of sample powder was weighed into a porcelain crucible, and was combusted in a muffle oven at 850 °C for 10 hours. The weight of processed samples was corrected according to the weights before and after the combustion. About 50 mg of combusted sample was weighed and transferred to a Teflon beaker. 1 mL of concentrated hydrochloric acid and 1.5 mL of concentrated hydrofluoric acid were added into the beaker for sample digestion. The capped beaker was then placed in a steel jacket and heated in an oven at 190 °C for 72 hours. Afterwards, the resulting solution was dried and 1 mL of HNO₃ was added twice and dried again. For complete dissolution of samples, 1.5 mL of HNO₃ was added and the capped beaker was replaced in the steel jacket in an oven for another 12 hours at 120 °C. Finally, the obtained sample solution was diluted using Mill-Q water and was ready for ICP-MS analysis. Rhodium was used as an internal standard during the ICP-MS measurement and its concentration in sample solution is 10 ppb. ICP-MS measurements were performed using an Element 2 (Thermo Fisher), and the analytical precision for trace elements was <10 %.

Major elements were analyzed using an ICP-AES (JY38S), and the analytical precision was better than 2 %. TOC were analyzed after removal of carbonate fractions with

10 % hydrochloric acid using Elemental Analyzer (Thermo Quest Italia. S.P.A). Results were corrected to the bulk weight of samples. Analytical precision was <0.2 %.

3 RESULTS

Trace elements (V, Cr, Ni, U, Mo, Th) and major element (Al₂O₃) concentrations and their enrichment factors relative to the Post Archean Average Shale (PAAS) in the samples of Jiulongwan and Baiguoyuan are presented in Table 1. Enrichment factors (EF) for U and Mo were calculated following Tribovillard et al. (2012): $X-EF=[(X/Al)_{sample}/(X/Al)_{PAAS}]$, where X and Al are the concentrations of element X and Al respectively.

The abundances for redox-sensitive trace elements V, Cr, Ni, U and Mo in the samples at Jiulongwan section show variation from 723–2 961 ppm (average 1 760 ppm), 84.5–401 ppm (average 194 ppm), 49.6–233 ppm (average 118 ppm), 14.6–39.5 ppm (average 21.5 ppm), and 48.0–463 ppm (average 123 ppm), respectively. The samples display significant enrichment for Mo and U with enrichment factors of 70–694 and 7–27. At Baiguoyuan, the concentrations for V, Cr, Ni, U and Mo are from 91.2–288 ppm (average 144 ppm), 58.8–118 ppm (average 89.2 ppm), 13.5–54.8 ppm (average 30.6 ppm), 1.9–3.2 ppm (average 2.6 ppm), and 1.4–5.5 ppm (average 2.6 ppm), respectively. The enrichment factors are 0.8–2.2 and 1.8–7.0 for U and Mo.

TOC abundances are listed together with the trace elements in Table 1. The TOC contents for the samples at Jiulongwan are from 3.2 %–9.2 %. No systematic change in TOC contents is observed across the section. At Baiguoyuan, the samples have lower TOC contents ranging from 0.7 %–1.2 %.

4 DISCUSSION

4.1 Mo-U Characteristics of the Doushantuo Black Shales and Their Implications

4.1.1 Background for the Mo-U covariation in marine sedimentary rocks

As redox-sensitive metals, the concentrations of U and Mo in marine sediments are widely used to evaluate the redox conditions of depositional environments (e.g. Perkins et al., 2008; Anbar et al., 2007; Tribovillard et al., 2006; Algeo, 2004). Under oxic seawater conditions, U and Mo occur as soluble U(VI) and Mo(VI); as certain redox threshold is reached, U(VI) and Mo(VI) can be reduced and incorporated into the sediments (Algeo and Tribovillard, 2009; Tribovillard et al., 2006). Therefore, sediments deposited in reducing water conditions usually contain elevated U and Mo contents (Tribovillard et al., 2006). However, the behavior of Mo and U in seawater are different in various aspects (Tribovillard et al., 2012; Algeo and Tribovillard, 2009). For example, Mo is strongly enriched in sediments if the bottom water is sulfidic while U enrichment in sediments shows no dependence of sulfidic bottom water conditions (Tribovillard et al., 2012; Zheng et al., 2000). An additional factor that would influence

the Mo and U enrichment patterns of sediments is the operation of the Mn shuttle within the water column. Crusius et al. (1996) suggested that intensive “particulate shuttle” of Mn oxyhydroxides in redox-stratified water column can “pump” Mo from surface water and facilitates Mo enrichment in sediments. Due to the different geochemistry in seawater between the two elements, the Mo and U characteristics in sedimentary rocks can offer interesting insights into the redox conditions in seawater and basin restriction during sediments deposition (Algeo and Tribovillard, 2009). Studies of modern open and restricted marine environments characteristic of different redox conditions show various patterns of sediment authigenic Mo-U covariations (Algeo and Tribovillard, 2009). As showed in Fig. 3A and Fig. 3B, in open marine environment like the continental margin in the eastern tropical Pacific, the enrichment factor of U (U-EF hereafter) and Mo (Mo-EF hereafter) of sediments are mainly influenced by the benthic redox conditions: in oxic conditions, the Mo-EF and U-EF of sediments generally exhibit low values; under suboxic conditions, U will be preferential-

ly enriched over Mo with Mo-EF/U-EF ratios well below the seawater Mo/U ratio; in anoxic environments, both U-EF and Mo-EF show stronger enrichment than oxic and suboxic conditions. Noticeably, the Mo-EF/U-EF ratios in anoxic sediments increase as U-EF and Mo-EF increase. In contrast, in restricted basin with sulfidic bottom water, the Mo-U co-variation patterns of sediments exhibit distinct characteristics. In highly restricted basin like the Black Sea, available Mo in water column can be rapidly consumed via burial in sediments, yet the replenishment of Mo in bottom water is limited due to basin restriction. Meanwhile, the U concentration in bottom water also decreases but to a less significant extent. Finally, the Mo-EF/U-EF ratio of sediments would evolve towards lower values as a result of low Mo/U ratios in the bottom water (Algeo and Tribovillard, 2009). Interestingly, in some mildly restricted basins like the Cariaco Basin, the operation of an active Mn oxyhydroxides shuttle would enhance Mo accumulation in sediments, leading to high Mo-EF/U-EF up to close/higher than three times of the seawater ratio.

Table 1 Trace elements (in ppm), Al₂O₃ and TOC content of the Doushantuo black shales

Samples	Height	V	Cr	Mn	Co	Ni	Mo	Th	U	TOC(%)	V/(V+Ni)	Ni/Co	Th/U	V/Cr	Al ₂ O ₃ (%)	Mo-EF	U-EF
Jiulongwan																	
JL-16-01	0.0	1 076	134	165	11.1	65.4	54.5	16.6	15.5	6.8 ^b	0.94	5.9	1.1	8.0	10.6	97.3	8.9
JL-16-02	0.0	1 424	155	206	14.9	88.7	208	18.2	17.7	5.6 ^b	0.94	6.0	1.0	9.2	11.5	340.7	9.4
JL-16-03	0.0	1 529	209	229	12.8	142	77.9	17.6	27.1	5.2 ^b	0.91	11.1	0.6	7.3	11.6	127.4	14.3
JL-16-04	0.0	1 569	151	285	15.2	170	463	17.6	35.9	5.0 ^b	0.90	11.1	0.5	10.4	12.6	694.4	17.4
JL-16-05	0.0	2 854	401	348	13.2	233	105	19.0	39.5	5.4 ^b	0.92	17.6	0.5	7.1	11.4	174.9	21.2
JL-16-06	0.0	2 022	263	251	14.7	128	70.2	19.3	26.9	4.7 ^b	0.94	8.7	0.7	7.7	12.8	103.9	12.9
JL-15-01	0.0	2 255	235	154	10.8	118	108	15.1	29.6	5.0 ^b	0.95	10.8	0.5	9.6	12.7	161.5	14.3
JL-15-02	0.6	1 959	265	240	12.6	130	63.6	16.3	18.8	4.6	0.94	10.3	0.9	7.4	12.6	95.7	9.1
JL-15-03	1.2	2 961	203	273	15.6	173	293	16.8	28.8	4.7	0.94	11.1	0.6	14.6	13.0	427.4	13.6
JL-15-04	1.8	2 157	197	225	13.7	104	57.5	16.0	15.7	4.6	0.95	7.6	1.0	10.9	12.9	84.3	7.4
JL-15-05	2.4	1 741	181	243	14.5	75.3	83.4	16.3	16.8	4.2	0.96	5.2	1.0	9.6	13.0	120.9	7.9
JL-15-06	3.0	2 367	212	240	15.3	124	92.6	16.8	19.3	3.2	0.95	8.1	0.9	11.2	13.8	126.8	8.5
JL-15-07	3.6	2 299	210	295	13.0	142	167	15.3	19.9	4.5	0.94	11.0	0.8	11.0	12.1	260.3	10.0
JL-15-08	4.2	2 034	184	229	14.7	109	48.0	16.2	14.6	4.9	0.95	7.4	1.1	11.1	12.9	70.2	6.9
JL-15-09	4.8	2 430	298	243	13.0	149	64.2	17.2	21.0	3.8	0.94	11.5	0.8	8.2	12.5	97.0	10.2
JL-15-10	5.4	1 413	175	255	14.0	71.9	67.3	15.8	15.3	3.4	0.95	5.1	1.0	8.1	12.7	99.9	7.3
JL-15-11	6.0	1 676	167	209	14.3	84.5	105	16.0	15.6	5.3	0.95	5.9	1.0	10.0	12.5	158.5	7.6
JL-15-12	6.6	1 850	175	252	14.1	115	232	19.3	21.0	4.4	0.94	8.1	0.9	10.6	11.7	373.5	10.9
JL-15-13	7.2	1 665	153	183	16.1	98.9	212	20.8	19.8	4.2	0.94	6.2	1.1	10.9	12.4	322.0	9.7
JL-15-14	7.8	1 653	184	204	14.1	108	95.9	20.8	23.2	4.9	0.94	7.7	0.9	9.0	12.1	150.0	11.7
JL-15-15	8.4	1 690	175	263	13.8	93.0	94.5	18.3	20.3	4.8	0.95	6.7	0.9	9.7	11.4	157.3	10.9
JL-15-16	9.0	1 205	178	195	12.4	75.0	118	20.9	24.1	3.9	0.94	6.1	0.9	6.8	11.5	193.0	12.7
JL-15-17	9.6	1 248	188	204	14.4	138	98.5	21.3	23.5	5.1	0.90	9.5	0.9	6.6	10.4	178.4	13.8
JL-15-18	10.2	1 435	174	282	11.8	131	96.6	16.9	24.0	5.9	0.92	11.1	0.7	8.3	10.8	168.8	13.5
JL-15-19	10.8	1 462	188	223	12.4	133	85.1	16.7	16.2	5.2	0.92	10.8	1.0	7.8	11.5	139.5	8.6
JL-15-20	11.4	1 718	191	280	12.6	159	108	13.9	18.9	5.5	0.92	12.6	0.7	9.0	10.4	197.4	11.1
JL-15-21	12.0	1 433	146	39.3	4.2	49.6	149	15.6	16.4	7.7	0.97	11.7	1.0	9.8	9.9	283.7	10.1
JL-15-22	12.6	723	84.5	365	7.7	109	70.9	8.6	17.4	7.9	0.87	14.1	0.5	8.5	10.5	127.9	10.1
JL-15-23	13.0	1 199	140	157	13.7	90.3	77.2	16.8	21.5	9.2	0.93	6.6	0.8	8.6	4.9	300.3	27.0
Baiguoyuan																	
skp-09	5.0	91.2	58.8	123	6.2	33.8	3.1	6.3	3.2	1.1 ^b	0.73	5.5	2.0	1.6	8.7	6.7	2.2
skp-10	6.0	288	118	71.3	6.7	44.7	5.5	8.5	1.9	1.2 ^b	0.87	6.6	4.5	2.4	15.0	7.0	0.8
skp-11	7.0	109	92.4	455	10.3	54.8	2.1	9.6	2.7	0.8 ^b	0.66	5.3	3.6	1.2	14.8	2.7	1.1
skp-12	8.0	119	95.7	47.0	3.3	16.1	2.3	10.0	2.5	0.9 ^b	0.88	4.9	4.0	1.2	14.8	3.0	1.0
skp-13	9.0	179	107	73.7	4.7	24.9	2.0	12.1	3.2	0.7 ^b	0.88	5.3	3.8	1.7	15.1	2.5	1.3
skp-14	10.0	94.7	76.8	72.0	4.9	26.1	1.6	8.6	2.5	0.7 ^b	0.78	5.4	3.5	1.2	13.6	2.2	1.1
skp-15	11.0	127	76.5	61.2	2.3	13.5	1.4	8.8	2.3	0.7 ^b	0.90	5.8	3.8	1.7	14.8	1.8	0.9

^a Datum for stratigraphic heights: base of the Doushantuo Member IV (samples from the Jiulongwan section), base of the lower phosphorite bed (samples from the Baiguoyuan section);

^b TOC data from Zhu B et al. (2013)

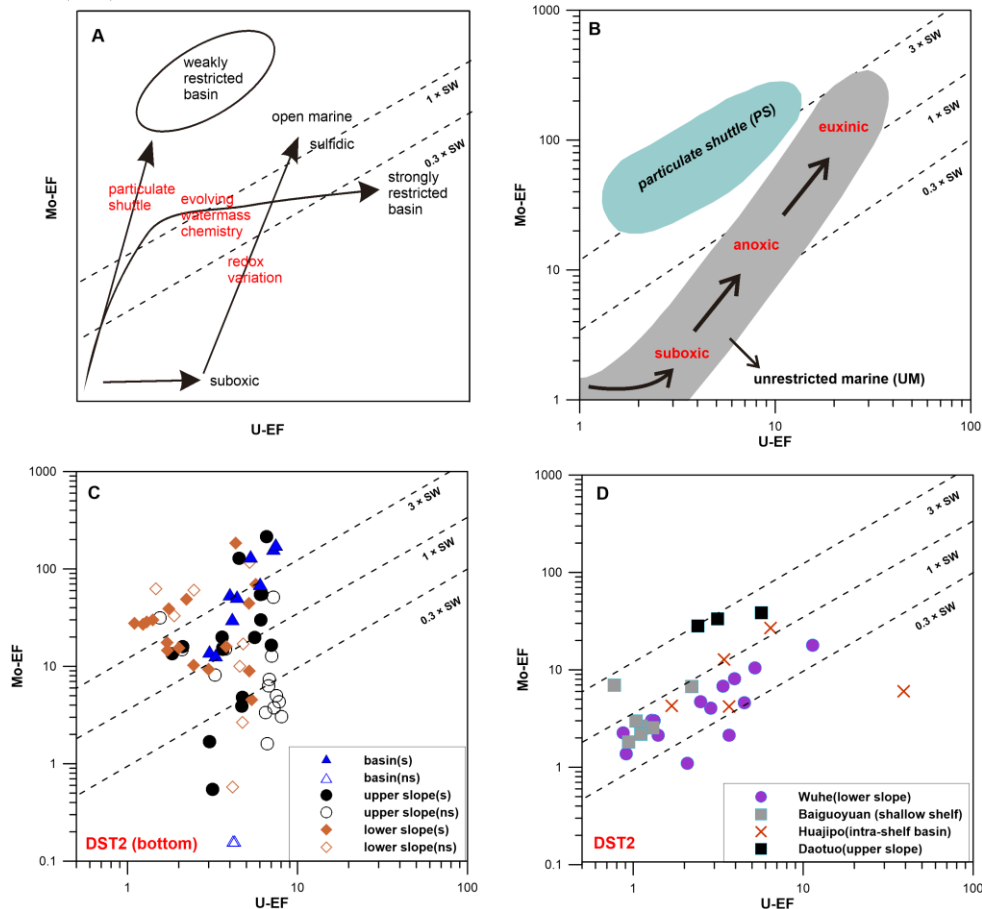


Figure 3 A. Model of enrichment patterns and changes in Mo-EF/U-EF ratios in response to the controls of redox variations, operation of a Mn shuttle and basin restriction (Algeo and Tribouillard, 2009). The heavy lines indicate the patterns of Mo-U covariation in different environments including open marine and restricted basins. B. General patterns of U-EF vs. Mo-EF covariation in modern marine environments (Algeo and Tribouillard, 2009). C. Patterns of U-EF vs. Mo-EF covariation in black shale of the bottom part of the Ediacaran DST2 of the Taoying (upper slope), Wuhe (lower slope), Yuanjia (basin) sections (Sahoo et al., 2012). Sulphidic(s) and non-sulphidic(ns) samples are indicated by solid and open symbols respectively based on Fe speciation data (Sahoo et al., 2012). The shales were interpreted to have documented an oxygenation event of the Ediacaran Ocean during their deposition. D. Patterns of U-EF vs. Mo-EF covariation in black shale above the bottom of the DST2 at Wuhe section (Sahoo et al., 2016), and black shales of DST2 from Baiguoyuan (shallow shelf, this study), Huajipo (intra-shelf basin, Kendall, 2008); Daotuo (upper slope, Zhai et al., 2016). At Baiguoyuan, the shales are from the lower DST2. At Huajipo and Daotuo, the samples, though limited, span the entire Doushantuo Member 2. In all figures, the dash lines indicate the multiples (0.3, 1 and 3) of the Mo:U ratio of present-day seawater.

4.1.2 Mo-U covariation in the Doushantuo Member II black shales

The Mo-U patterns of sediments of various settings shown in Fig. 3A and 3B provide a basis for evaluation of the depositional environment of the Doushantuo black shales. However, given that the Mo and U inventories in the Ediacaran ocean may differ from that of the Modern Ocean, caution must be taken when applying these figures to evaluate the redox and oceanographic conditions of the Doushantuo black shales during their deposition. As the UM (unrestricted marine) zone and the PS (particulate shuttle) zone in Fig. 3B are based on Mo-U data of modern marine sediments, direct application of them to the Ediacaran black shales can be arbitrary. Nevertheless, the fundamental principles behind the Mo-U covariation diagram, i.e. the different mechanisms of Mo and U enrichments in sediments under different redox conditions, the influences on Mo and U concentrations of seawater by restricted environments and bottom water stagnancy, should be still

valid. In this sense, to assess the redox conditions of the Doushantuo black shales, the main focus should be the differences of Mo-U covariation patterns of different sample sets in the U-EF vs. Mo-EF diagrams, rather than the absolute positions of the sample plots with respects to the UM and PS zones. Figure 3C and 3D show the compiled Mo-U diagrams of the Doushantuo Member II (DST2 hereafter) black shales from a range of sedimentary facies including shallow shelf (Baiguoyuan), intra-shelf basin (Huajipo), upper slope (Taoying, Daotuo), lower slope (Wuhe) and deep basin (Yuanjia) (Fig. 2B). As Fe speciation data are available for some sections (Taoying, Wuhe and Yuanjia; Sahoo et al., 2016; 2012), the combined Mo-U and Fe speciation data render the possibilities to investigate how Mo-EF and U-EF varied in response to changes in redox conditions and possibly, basin restriction during the deposition of these shales. It is noticeable that an oxygenation event in the anoxic Ediacaran ocean happened during deposition of the bottommost part of the DST2, as

documented in the shales at the Wuhe, Yuanjia and Taoying sections (Sahoo et al., 2012). Following the oxygenation, the ocean returned to persistent euxinia and ferruginous conditions till the deposition of the Doushantuo Member III (Sahoo et al., 2016; 2012). The overall marine redox conditions are known to regulate the availabilities of redox-sensitive elements (RSE) in seawater (e.g. Reinhard et al., 2013), and would also influence the interpretation of the Mo-U data. Therefore, in the following discussion, the DST2 shales that were interpreted to have documented the oxygenation event at the bottom of the DST2, and the other compiled data from the DST2 will be discussed separately.

(1) Mo-U patterns of shales of the bottom DST2

Figure 3C shows the Mo-U diagrams of shales from the bottom of the DST2 from the Taoying, Wuhe and Yuanjia sections, with solid symbols indicating sulfidic condition (Sahoo et al., 2012). At the basinal Yuanjia section, Fe speciation data indicated most shales were deposited in a sulphidic bottom water condition. The high Mo-EF and U-EF values are consistent with a highly oxic ocean with elevated aqueous Mo and U in seawater (Sahoo et al., 2012; Fig. 3C). Noticeably, the Mo-EF/U-EF ratios increase from 1 to above 3 times that of modern seawater as U-EF and Mo-EF increase. The increase in Mo-EF/U-EF ratios as total U and Mo enrichment factors increase is typical of modern marine sediments deposited in open marine environments (Fig. 3A, 3B). In comparison, sections from the upper and the lower slope (Taoying, Wuhe) exhibit large scatter in the Mo-U crossplots with Mo-EF, U-EF and Mo-EF/U-EF values covering wide ranges (Fig. 3C). As meter-scale variations in both Fe_{HR}/Fe_T and Fe_{pyrite}/Fe_{HR} were observed in these shales and were interpreted to reflect dynamic, redox fluctuations alternating between oxic, suboxic, and anoxic local environments (Sahoo et al., 2012), the highly scattered data and the wide range of Mo-EF/U-EF ratios for the shales of the slope sections probably reflect highly variable benthic redox conditions. Some of the samples are characterized by high Mo-EF values but relatively low U-EF with Mo-EF/U-EF ratios above the $3 \times SW$ line (Fig. 3C). This pattern is analogous to that observed in the modern Cariaco Basin (Algeo and Tribouillard, 2009), and therefore is likely to reflect the operation of a Mn oxyhydroxide shuttle.

(2) Mo-U patterns of shales of the rest of the DST2

Following the deposition of the bottom of the DST2, the ocean was predominantly anoxic till deposition of the Doushantuo Member III (Sahoo et al., 2016). At the Wuhe section (lower slope), the shales above the bottom of the DST2 were all deposited in euxinic bottom water conditions (Sahoo et al., 2016). Compared to the bottom DST2 shales from the basinal Yuanjia section that is characterized by persistent local euxinia (Fig. 3C), the Mo-U patterns in these shales are significantly different: the Mo-EF values are much lower with very low U-EF values near 1 shown, and the Mo-EF/U-EF values are all below the $1 \times SW$ line (Fig. 3D). The low U-EF and Mo-EF are consistent with low concentrations of U and Mo in seawater in a predominately anoxic ocean during this period (Sahoo et al., 2016). However, at the upper slope Daotuo section, the Mo-U patterns of black shales are significantly different: the U-EF values of Daotuo are within the range of the U-

EF values at Wuhe; the Mo-EF and the Mo-EF/U-EF ratios are however significantly higher at the Daotuo section (Fig. 3D). As the shales at Daotuo were interpreted to have deposited in an anoxic bottom water (Zhai et al., 2016), the differences in the Mo-U patterns can hardly be caused by different redox conditions at the two sites. There are two possible explanations for the different Mo-U patterns at the two sections. First, the elevated Mo-EF and Mo-EF/U-EF values simply reflect higher Mo concentration in seawater at the site of Daotuo. Alternatively, the values reflect the influences of a Mn shuttle similar to that of the modern Cariaco Basin. Mo-TOC patterns of anoxic marine sediments are known to be scaled to the Mo concentrations of surrounding seawater (Algeo and Lyons, 2006, see section 5.3 for more details), thus the Mo-TOC patterns for the DST2 black shales at Wuhe and Daotuo seem to support the first explanation that the shales at the two sections sequestered Mo from seawater characterized by different Mo concentrations (Fig. 5A). Given the different paleogeographic settings of the two sections (upper slope for Daotuo and lower slope for Wuhe), the differences in Mo-TOC and Mo-U patterns probably reflect higher Mo concentration of seawater at the upper slope section and may record heterogeneous aqueous Mo in seawater at the two sites. This is somewhat similar to the aqueous profiles of Mo observed in modern restricted basin like the Black Sea and the Cariaco Basin where the vertical gradient of dissolved Mo showed a decrease from surface to bottom water (Algeo and Tribouillard, 2009). However, due to limited data at Daotuo and too many unknown variables, the existence of heterogeneities of aqueous Mo at the two sites still need to be tested by further work.

Paleogeographic reconstruction indicated a barrier existed between the intra-shelf basin and the open ocean during deposition of the Doushantuo Formation (Jiang et al., 2011; Fig. 1A, 1B). Meanwhile, recent studies suggested that the intra-shelf basin was redox stratified during deposition of the Doushantuo Member II and Member III, with oxic surface water and anoxic (ferruginous and sulfidic) deep water (Fan et al., 2014, Li et al., 2010). The redox stratification and the geographic setting of the intra-shelf basin are somewhat analogues to that of modern anoxic restricted basins like the Black Sea. In the highly restricted Black Sea, the bottom water is characterized by much lower aqueous Mo and Mo/U ratios than the open ocean, and the sediments tend to exhibit lower Mo-EF/U-EF values than anoxic open marine sediments (Algeo and Tribouillard, 2009; Fig. 3A). The Huajipo section in the Three Gorges area was deposited in deep water within the intra-shelf basin (Fig. 2B). In comparison to the DST2 shales of open marine environments, the data points of Huajipo fall between the ranges of Daotuo and Wuhe (Fig. 3D). If a vertical gradient did exist in the ocean, as discussed above, the Mo-U patterns of the Daotuo shales may better track the Mo and U characteristics of shallow seawater that had connection to the intra-shelf basin. In this case, the different Mo-U patterns of Daotuo and Huajipo probably suggest the aqueous Mo in the bottom water of the intra-shelf basin was lower than the open ocean. However, as discussed above, the existence of heterogeneities of aqueous Mo at different water depth still needs to be tested by further work. Nevertheless, the Mo-U pattern at Huajipo resembles that of

sediments in highly restricted environment shown in Fig. 3A, i.e. no significant increase in Mo-EF and decrease in Mo-EF/U-EF as U-EF increase. Noticeably, the profoundly high U-EF (>20) but very low U-EF/Mo-EF (<0.3 times that of present-day seawater) seen in one sample point is similar to that of the Black Sea sediments (Algeo and Tribovillard, 2009). These observations indicate that basin restriction may have happened during deposition of these shales. This interpretation is compatible with a previous mineralogical study that suggested the DST2 was deposited in a highly restricted environment in the intra-shelf basin (Bristow et al., 2009).

In comparison to the shales at Huajipo and other sections, the U-EF and Mo-EF values of the Baiguoyuan shales are generally lower (Fig. 3D), indicating a less reducing bottom water condition than the Huajipo section. Most of the U-EF values are near 1 with Mo-EF/U-EF below the $1 \times SW$ line (Fig. 3D). The Mo-U patterns of the shales closely resemble that of the oxic-suboxic sediments of the southern and central California shelf margin (Algeo and Tribovillard, 2009). According to the model of Fan et al. (2014), during deposition of the Doushantuo Member II and Member III, seawater of the intra-shelf was strongly redox stratified with oxic surface water and anoxic deep water, and the Baiguoyuan section was located above/near the chemocline. Our Mo-U data of the Baiguoyuan shales are consistent with the interpretation of Fan et al. (2014). Moreover, given the paleogeographic settings of the Huajipo and Baiguoyuan sections (Fig.1B), the contrasting Mo-U patterns at the two sections reflect different redox conditions at different water depths, which is also compatible with the stratified model of the intra-shelf basin.

Since samples from the Huajipo and Daotuo sections span the whole DST2, thus a few samples (one from Huajipo and one from Daotuo) from the lower part of the DST2 at these sections may have deposited during the oxygenation event. Nevertheless, we consider our primary conclusion is unlikely to be dramatically altered, as we focused on the overall features of the data sets at each section in the above discussion.

4.1.3 Mo-U covariation in the Doushantuo Member IV black shales

For the Doushantuo Member IV, we can only obtain Mo-U data from the intra-shelf basin sections including the Jiulongwan section, an drill core section ~5 km away from Jiulongwan, and one slope section (Wuhe) (Fig. 4; Sahoo et al., 2016; Kendall et al., 2015). Shales from the intra-shelf sections display similar Mo-U patterns characterized by high U and Mo enrichment factors with Mo-EF values up to several hundreds. All data are plotted above the $1 \times SW$ line with some data points well above the $3 \times SW$ line (Fig. 4). The similarities in Mo-U patterns at the sections indicate no significant lateral differences in depositional conditions during sedimentation of the shales. Although a growing body of evidence shows that the majority of the ocean was oxygenated at the end of the Doushantuo time (Sahoo et al., 2016; Kendall et al., 2015; Scott et al., 2008), the local redox condition of the bottom water for these shales was sulfidic as evidenced by Fe speciation data (Kendall et al., 2015; Li et al., 2010). A sulfidic

bottom water condition is in concordance with the high enrichment factors for both U and Mo of the shales in Fig. 4.

At the slope Wuhe section, the Doushantuo Member IV shales also exhibit high U enrichment factors and are all above the $1 \times SW$ line in the Mo-U diagram, but very high Mo-EF values (>300) seen in the intra-shelf basin section are not observed (Fig.4).

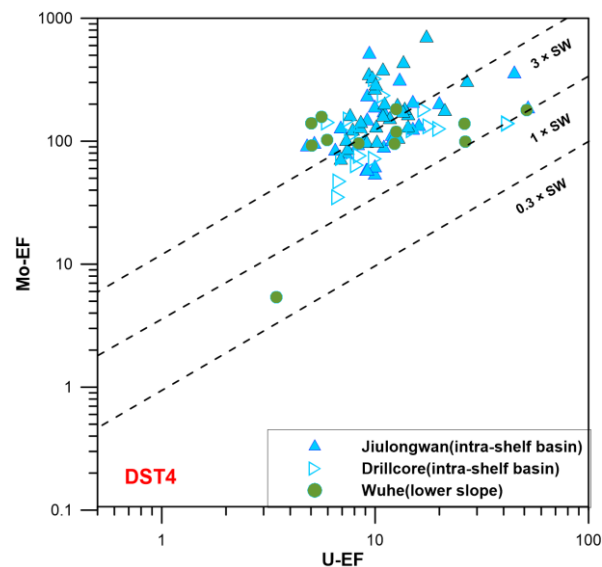


Figure 4 Patterns of U-EF vs. Mo-EF covariation in black shale of the Ediacaran Doushantuo Member IV from the intra-shelf basin sections including the Jiulongwan section (this study, Kendall et al., 2015), a drill core section from the Three Gorges area ~5 km away from Jiulongwan (Kendall et al., 2015), and the Wuhe section (lower slope, Sahoo et al., 2016). The dash lines indicate the multiples (0.3, 1 and 3) of the Mo:U ratio of the present-day seawater.

Besides, some shales from the intra-shelf basin sections have significantly higher Mo-EF/U-EF ratios than that of the slope section (Fig.4). Since the shales from the slope section were also deposited in sulfidic bottom water condition (Sahoo et al., 2016), the higher Mo-EF/U-EF ratios seen in the intra-shelf basin sections may reflect the operation of additional factors that enhance Mo enrichment in the sediments. In the modern Cariaco Basin, active redox cycling of Mn is considered to deliver abundant Mo to sediments and finally results in high Mo-EF/U-EF ratios in sediments (Algeo and Tribovillard, 2009; Fig. 3A, 3B). This mechanism could be a possible explanation for the elevated Mo-EF/U-EF ratios of the Doushantuo Member IV shales. In a recent study of Mo isotopes of the Doushantuo IV black shales at Jiulongwan, the Mn shuttle was invoked as a possible explanation for the light Mo isotopic compositions in some of these shales (Kendall et al., 2015). In that scenario, Fe and Mn oxyhydroxide particles formed near the chemocline would preferentially absorb the lighter isotopes of Mo during sinking. And the absorbed Mo would be sequestered in sediments upon releasing via reduction of Fe-Mn oxides below the chemocline (Kendall et al., 2015).

4.2 OTHER REDOX-SENSITIVE ELEMENTS AND DIAGNOSTIC RATIOS

The concentrations of redox-sensitive trace elements like V, Ni, Cr, U and their ratios in marine sediments can offer useful information regarding the local paleo-redox conditions (e.g. Zhou and Jiang, 2009, Guo et al., 2007). For instance, previous studies proposed that V/Cr ratios lower than 2, between 2 to 4.25 and larger than 4.25 indicate oxic, suboxic and anoxic conditions, respectively (Jones and Manning, 1994). Meanwhile, V/(V+Ni) ratio > 0.60, Ni/Co ratio > 7, and Th/U ratios < 2 usually indicate anoxic environment (Rimmer, 2004, Wignall and Twitchett, 1996, Hatch and Leventhal, 1992).

For the Doushantuo Member IV shales at Jiulongwan, all samples display high V/Cr ratios (7–15), higher V/(V+Ni) ratios (0.87–0.97), and low Th/U ratios (0.5–1.1) (Table 1). Most samples have high Ni/Co ratios with a few displaying Ni/Co ratios slightly lower than the threshold (Table 1). The trace elements characteristics point to an overall anoxic local environment during deposition of the Doushantuo Member IV, which is consistent with the interpretation based on Mo-U patterns (section 5.1.2) and iron speciation data by Li et al. (2010).

For the Doushantuo Member II samples at Baiguoyuan, the V/Cr and Ni/Co ratios are lower (1.1–2.5 and 4.7–6.6 respectively) with Th/U ratios ranging from 2.0 to 4.4, suggesting of an oxic depositional environment for these rocks. However, V/(V+Ni) ratios of 0.7–0.9 point to an opposite conclusion. The inconsistency between different redox trace-elements ratios have also been documented in Rimmer (2004), in which the authors reported that V/(V+Ni) ratios tend to predict lower oxygen conditions than other redox indices, and Ni/Co and V/Cr ratios showed fairly agreement with other redox indices inferred by carbon, sulfur and iron relationships. Therefore, application of the V/(V+Ni) ratios for sedimentary rocks may require some cautions and should be more focused on the relative differences within a data set rather than some specific thresholds (Rimmer, 2004). Nevertheless, oxic depositional environment indicated by the other more promising ratios

(Ni/Co, V/Cr) is consistent with the Mo-U data and the observation that the samples have low enrichment factor for Mo, U and other redox-sensitive elements (Table 1).

4.3 MO VS. TOC FOR THE DOUSHANTUO BLACK SHALES

Studies of modern restricted marine environment with anoxic bottom water like the Black Sea and the Cariaco Basin indicate the aqueous Mo concentrations in bottom seawater of these basins are sensitive to the extent of basin restriction (Algeo and Lyons, 2006). Highly restricted basins show rapid decrease in aqueous Mo contents with depth while only slight decrease has been observed in mildly restricted basins (Algeo and Lyons, 2006). Finally, the Mo patterns of water column have a major influence on the Mo characteristics in sediments. In an extensive study of modern restricted environments by Algeo and Lyons (2006), the authors documented that Mo and TOC contents of sediments are correlated with each other in individual restricted basin, with the slopes of the data array in the Mo-TOC diagrams varying among different basin. Interestingly, the slope seems to be positively correlated with the Mo concentration in deep water, which is greatly regulated by the residence time of deep water (i.e. basin restriction).

Figure 5B shows the Mo-TOC patterns of several modern restricted environments. The most restricted Black Sea shows the lowest slope (ca. 4.5). As basin restriction decreases, the slope increases with highest value of ca. 45 as shown in the mildly restricted Saanich inlet. These observations provide the basis for using Mo/TOC characteristics in marine sediments to evaluate the Mo availability in deep water as well as the extent of basin restriction (e.g. Algeo and Rowe, 2012; McArthur et al., 2008; Scott et al., 2008). Figure 5B also shows the compiled Mo-TOC data of the Doushantuo Member IV shales of the Jiulongwan section (intra-shelf basin), a drill core section ~5 km to Jiulongwan, and the Wuhe section (lower slope).

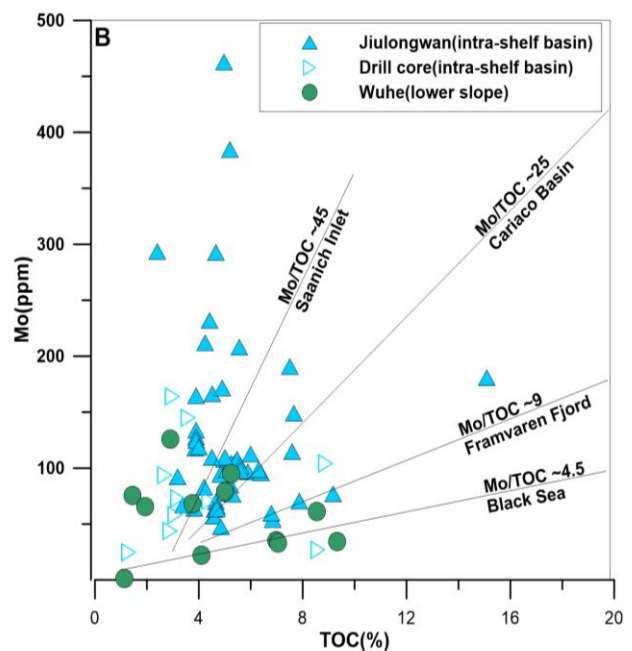
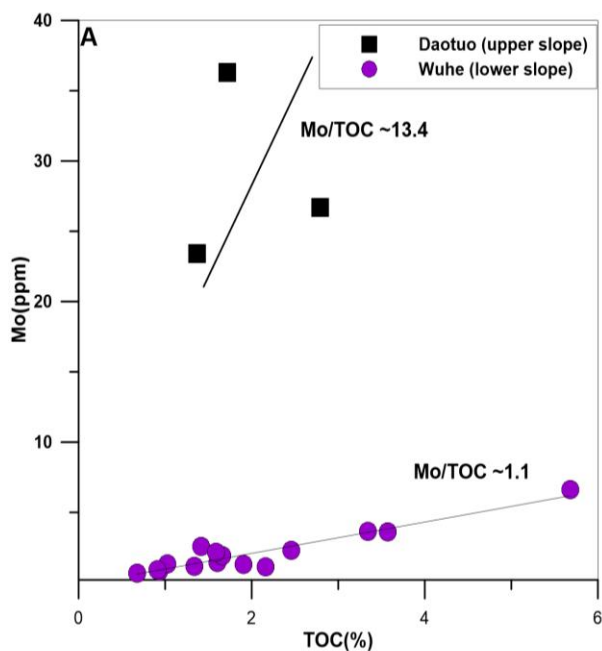


Figure 5 A: TOC-Mo diagram for the Doushantuo Member II black shale at the Wuhe and Daotuo sections. Data source: Wuhe (Sahoo et al., 2016); Daotuo (Zhai et al., 2016). Note the data of Wuhe eliminate those of shales above the bottom part that represent an oxygenation event of Ediacaran ocean (Sahoo et al., 2016). **B:** Mo-TOC diagram for the Doushantuo Member IV black shale from the intra-shelf basin sections including the Jiulongwan section (this study, Kendall et al., 2015), a drill core section ~5 km away from Jiulongwan (Kendall et al., 2015), and the Wuhe section (lower slope, Sahoo et al., 2016). Four reference lines representing Mo-TOC characteristic in modern restricted marine environments are also shown in the figure (Algeo and Lyons, 2006; Algeo and Rowe, 2009). Note the Mo/TOC ratios are in units of ppm/%.

The Mo-TOC patterns in the shales indicate that the black shales were probably deposited in water column with Mo In Fig. 5B, most data from the intra-basin sections (Jiulongwan and the drill core section) display high Mo/TOC ratios and cluster near/above the line for the Saanich inlet, with a few data points below the Cariaco Basin line. concentration similar to or higher than that of the Saanich inlet, in which the deep water have aqueous Mo concentrations only slightly lower than that of modern seawater (Algeo and Lyons, 2006). The Saanich inlet is only weakly restricted with renewal time of deep waters of <2 yr (Algeo and Lyons, 2006). In this case, if the open marine seawater had Mo concentration similar to that of today during Ediacaran, the Mo-TOC pattern for the shales would suggest that the intra-shelf basin was well connected to the open ocean during deposition of the Doushantuo IV shales. The exact Mo content in open marine environment during deposition of these rocks is hard to assess, but some estimate can be made based on available geochemical evidences. The Mo concentration in modern seawater is regulated by two major factors: the fluvial input which transports Mo by oxidation weathering of continental crusts, and the area of reducing seafloor where burial fluxes of Mo exceed those in oxygenated settings by several orders of magnitude (Reinhard et al., 2013, Scott et al., 2008, Algeo, 2004). Previous studies have suggested the Mo inventory in the Ediacaran ocean have significantly expanded periodically (Sahoo et al. 2016, 2012; Kendall et al., 2015; Scott et al., 2008), but Mo isotope evidences indicate the oxidation of the deep ocean may not reach the present-day level until early Cambrian (Chen et al., 2015), indicating the Mo concentration in Ediacaran ocean is unlikely higher than that of the modern ocean. Therefore, given the Mo-TOC patterns for the samples, the Doushantuo Member IV shales were most likely deposited in an environment with good connection to the open ocean despite the geographic setting. This interpretation is consistent with the study by Bristow et al. (2009), who suggested that the Doushantuo Member IV at Jiulongwan were deposited in a relatively open marine environment on the basis of mineralogical analysis. Besides, the Mo-TOC patterns of the DST4 black shale from the slope Wuhe section also support this interpretation. The Mo/TOC ratios at both the intra-shelf sections and the slope section cover similar ranges (Fig. 5B), indicating no significant differences in aqueous Mo at both sites. As the Jiulongwan and the nearby drill core sections were deposited in relatively deep water of the intra-shelf basin (Fig. 2B), the Mo-TOC characteristics of the DST4 black shale from the intra-shelf and the slope sections strongly support no significant drawdown of aqueous Mo in the deep water of the intra-shelf basin, and thereby no significant deep water stagnancy and basin restriction during deposition of these shales.

When applying the Mo-TOC patterns to evaluate basin restriction for sediments, an important premise is that the sediments should be deposited in anoxic environments. Previous studies indicate that modern and Phanerozoic sediments

accumulated in oxic-suboxic environments display low Mo/TOC ratios yet the ratios do not reflect low Mo availability in seawater (Tribovillard et al., 2006, Algeo and Maynard, 2004). In this case, the Mo-TOC data of the Baiguoyuan samples, which may have deposited in oxic-suboxic conditions (see Section 5.1, 5.2), cannot provide information regarding the Mo contents of surrounding seawater and the extent of basin restriction.

5 CONCLUSIONS

This study presents trace elements and TOC data of the Ediacaran Doushantuo black shales at two intra-shelf sections in Hubei Province. Data of the two sections and previously published trace elements, TOC, and Fe speciation data from other 6 sections covering a variety of sedimentary facies from intra-shelf to basin described dynamic redox and oceanographic conditions during deposition of the Ediacaran Doushantuo Formation on the Yangtze platform.

At the slope and basinal sections, distinct types of Mo-U patterns between black shales from the bottom and the rest part of the Doushantuo Member II are consistent with a shift from a predominately oxic to a predominately anoxic ocean. At the intra-shelf sections, Mo-U patterns of the Doushantuo Member II shales reflect basin restriction may have happened in the intra-shelf basin. Mo-U patterns documented in the Doushantuo Member II black shales at the Baiguoyuan section likely reflect oxic-suboxic bottom water condition, which is in concordance with the model of redox stratified water in the intra-shelf basin.

The Doushantuo Member IV shales from two intra-shelf sections (Jiulongwan and a drill core section nearby) exhibit Mo-U patterns indicative of anoxic bottom water condition for the shales. More prominent Mo enrichment and higher Mo-EF/U-EF ratios at the intra-shelf sections than the slope Wuhe section indicate that the operation of a Mn particulate shuttle in the intra-shelf basin. High Mo/TOC ratios of the Doushantuo Member IV shales at intra-shelf sections, in combination with similar Mo-TOC patterns of the Doushantuo Member IV shales from both intra-shelf and slope sections, indicate the intra-shelf basin was well connected to the open ocean during deposition of the Doushantuo Member IV shales.

ACKNOWLEDGMENTS

This work was supported by grants from National Natural Science Foundation of China (41302018, 41230102, 41203021), National 973 project (2013CB835000), the Foundation of State Key Laboratory of Petroleum Resources and Prospecting, China University of Petroleum, Beijing (No. PRP/open-1305) and Ph.D. Programs Foundation of Ministry of Education of China (20130094120008). The final publication is available at Springer via <http://dx.doi.org/10.1007/s12583-017-0907-5>.

REFERENCES CITED

- Algeo, T. J., Lyons, T. W., 2006. Mo-Total Organic Carbon Covariation in Modern Anoxic Marine Environments: Implications for Analysis of Paleoredox and Paleohydrographic Conditions. *Paleoceanography*, 21(21): 279–298
- Algeo, T. J., Maynard, J. B., 2004. Trace-Element Behavior And Redox Facies in Core Shales of Upper Pennsylvanian Kansas-Type Cyclothems. *Chemical Geology*, 206(3–4): 289–318
- Algeo, T. J., Rowe, H., 2012. Paleocyanographic Applications of Trace-Metal Concentration Data. *Chemical Geology*, 324–325: 6–18
- Algeo, T. J., Tribouillard, N., 2009. Environmental Analysis of Paleocyanographic Systems Based on Molybdenum-Uranium Covariation. *Chemical Geology*, 268(3–4): 211–225
- Algeo, T. J., 2004. Can Marine Anoxic Events Draw Down the Trace Element Inventory of seawater? *Geology*, 32(12): 1057–1060
- Anbar, A. D., Duan, Y., Lyons, T. W., et al., 2007. A Whiff of Oxygen Before the Great Oxidation Event? *Science*, 317(5846): 1903–1906
- Bjerrum, C. J., Canfield, D. E., 2011. Towards a Quantitative Understanding of the Late Neoproterozoic Carbon Cycle. *Proceedings of the National Academy of Sciences*, 108(14): 5542–5547
- Brasier, M., Antcliffe, J., 2004. Decoding the Ediacaran Enigma. *Science*, 305(5687): 1115–1117
- Bristow, T. F., Kennedy, M. J., Derkowski, A., et al., 2009. Mineralogical Constraints on the Paleoenvironments of the Ediacaran Doushantuo Formation. *Proceedings of the National Academy of Sciences*, 106(32): 13190–13195
- Canfield, D. E., Poulton, S. W., Narbonne, G. M., 2007. Late-Neoproterozoic Deep-Ocean Oxygenation and the Rise of Animal Life. *Science*, 315(5808): 92–95
- Chen, X., Ling, H. F., Vance, D., et al., 2015. Rise To Modern Levels of Ocean Oxygenation Coincided with the Cambrian Radiation of Animals. *Nature Communications*, 6: 7142
- Condon, D., Zhu, M. Y., Bowring, S., et al., 2005. U-Pb Ages from the Neoproterozoic Doushantuo Formation, China. *Science*, 308(5718): 95–98
- Crusius, J., Calvert, S., Pedersen, T., et al., 1996. Rhenium and Molybdenum Enrichments in Sediments as Indicators of Oxidic, Suboxic and Sulfidic Conditions Of Deposition. *Earth and Planetary Science Letters*, 145(1–4): 65–78
- Fan, H., Zhu, X., Wen, H., et al., 2014. Oxygenation of Ediacaran Ocean Recorded by Iron Isotopes. *Geochimica Et Cosmochimica Acta*, 140: 80–94
- Fike, D. A., Grotzinger, J. P., Pratt, L. M., et al., 2006. Oxidation of the Ediacaran Ocean. *Nature*, 444(7120): 744–747
- Guo, Q., Shields, G. A., Liu, C., et al., 2007. Trace Element Chemostratigraphy of Two Ediacaran–Cambrian Successions in South China: Implications for Organosedimentary Metal Enrichment And Silicification in the Early Cambrian. *Palaeoogeography, Palaeooclimatology, Palaeoecology*, 254(1–2): 194–216
- Halverson, G. P., Dudás, F. Ö., Maloof, A. C., et al., 2007. Evolution of the $^{87}\text{Sr}/^{86}\text{Sr}$ Composition of Neoproterozoic seawater. *Palaeoogeography, Palaeooclimatology, Palaeoecology*, 256(3–4): 103–129
- Halverson, G. P., Wade, B. P., Hurtgen, M. T., et al., 2010. Neoproterozoic Chemostratigraphy. *Precambrian Research*, 182(4): 337–350
- Hatch, J. R., Leventhal, J. S., 1992. Relationship Between Inferred Redox Potential of the Depositional Environment and Geochemistry of the Upper Pennsylvanian (Missourian) Stark Shale Member of the Dennis Limestone, Wabaunsee County, Kansas, U.S.A. *Chemical Geology*, 99(1–3): 65–82
- Jiang, G., Shi, X., Zhang, S., et al., 2011. Stratigraphy and Paleogeography of the Ediacaran Doushantuo Formation (Ca. 635–551Ma) in South China. *Gondwana Research*, 19(4): 831–849
- Jones, B., Manning, D. A. C., 1994. Comparison of Geochemical Indexes Used for the Interpretation of Paleoredox Conditions in Ancient Mudstones. *Chemical Geology*, 111(1–4): 111–129
- Kendall, B., Komiya, T., Lyons, T. W., et al., 2015. Uranium and Molybdenum Isotope Evidence for An Episode of Widespread Ocean Oxygenation During the Late Ediacaran Period. *Geochimica Et Cosmochimica Acta*, 156:173–193.
- Kendall, B. S., 2008. Rhenium-Osmium Geochronology of Precambrian Organic-Rich Sedimentary Rocks, Systematics and Applications: [Dissertation]. Edmonton, Alberta, University Of Alberta.59
- Kendall, B., Creaser, R. A., Selby, D., 2009. ^{187}Re - ^{187}Os Geochronology of Precambrian Organic-Rich Sedimentary Rocks. *Geological Society, London, Special Publications*, 326(1): 85–107
- Knoll, A. H., Walter, M. R., Narbonne, G. M., et al., 2004. A New Period for the Geologic Time Scale. *Science*, 305(5684): 621–622
- Knoll, A., Walter, M., Narbonne, G., et al., 2006. The Ediacaran Period: A New Addition to the Geologic Time Scale. *Lethaia*, 39(1): 13–30
- Li, C., Love, G. D., Lyons, T. W., et al., 2010. A Stratified Redox Model for the Ediacaran Ocean. *Science*, 328(5974): 80–83
- Li, C., Zhu, M., Chu, X., 2016. Atmospheric and Oceanic Oxygenation and Evolution of Early Life on Earth: New Contributions From China. *Journal of Earth Science*, 27(2): 167–169
- Liu, P. J., Yin, C. Y., Gao, L. Z., et al., 2009. New Material Of Microfossils From The Ediacaran Doushantuo Formation in the Zhangcunping Area, Yichang, Hubei Province and Its Zircon SHRIMP U-Pb Age. *Chinese Science Bulletin*, 54(6): 1058–1064
- Liu, P., Chen, S., Zhu, M., et al., 2014. High-Resolution Biostratigraphic and Chemostratigraphic Data from the Chenjiayuanzi Section of the Doushantuo Formation in the Yangtze Gorges Area, South China: Implication for Subdivision and Global Correlation of the Ediacaran System. *Precambrian Research*, 249(4): 199–214
- Liu, P., Yin, C., Chen, S., et al., 2013. The Biostratigraphic Succession of Acanthomorphic Acritarchs of the Ediacaran Doushantuo Formation in the Yangtze Gorges Area, South China and Its Biostratigraphic Correlation with Australia. *Precambrian Research*, 225: 29–43
- Lyons, T. W., Reinhard, C. T., Planavsky, N. J., 2014. The Rise of Oxygen in Earth's Early Ocean and Atmosphere. *Nature*, 506(7488): 307–315
- McArthur, J. M., Algeo, T. J., Van De Schootbrugge, B., et al., 2008. Basinal Restriction, Black Shales, Re-Os Dating, and the Early Toarcian (Jurassic) Oceanic Anoxic Event. *Paleoceanography*, 23.PA4217, doi:10.1029/2008PA001607
- Mccall, G., 2006. The Vendian (Ediacaran) In the Geological Record: Enigmas in Geology's Prelude to the Cambrian Explosion. *Earth-Science Reviews*, 77(1–3): 1–229
- Mcfadden, K. A., Huang, J., Chu, X., et al., 2008. Pulsed Oxidation and Biological Evolution in the Ediacaran Doushantuo Formation. *Proceedings of the National Academy of Sciences*, 105(9): 3197–3202
- Mi, T. W., Lin, L., Pang, Y. C., et al., 2010. The Sequence Stratigraphy and Genesis of Phosphorites of Doushantuo Formation at Baiguoyuan, Yichang, Hubei. *Acta Sedimentologica Sinica*, 28(3): 471–480 (in Chinese with English abstract)
- Och, L. M., Cremonese, L., Shields-Zhou, G. A., et al., 2015. Palaeocyanographic Controls on Spatial Redox Distribution over the Yangtze Platform during the Ediacaran–Cambrian Transition. *Sedimentology*, 63(2): 378–410
- Perkins, R. B., Piper, D. Z., Mason, C. E., 2008. Trace-Element Budgets in the Ohio/Sunbury Shales of Kentucky: Constraints on Ocean Circulation and Primary Productivity in the Devonian–Mississippian Appalachian Basin. *Palaeoogeography, Palaeooclimatology, Palaeoecology*, 265(1–2): 14–29
- Reinhard C. T., Planavsky N. J., Robbins L. J., et al. 2013. Proterozoic Ocean Redox and Biogeochemical Stasis. *Proceedings Of The National Academy of Sciences of the United States of America*, 110(14): 5357–62.
- Ries, J. B., Fike, D. A., Pratt, L. M., et al., 2009. Superheavy Pyrite ($^{34}\text{S}_{\text{pyr}} > ^{34}\text{S}_{\text{CAS}}$) In the Terminal Proterozoic Nama Group, Southern Namibia: a Consequence of Low Seawater Sulfate at the Dawn Of Animal Life. *Geology*, 37(8): 743–746
- Rimmer, S. M., 2004. Geochemical Paleoredox Indicators in Devonian–Mississippian Black Shales, Central Appalachian Basin (USA). *Chemical Geology*, 206(3–4): 373–391
- Sahoo, S. K., Planavsky, N. J., Jiang, G., et al., 2016. Oceanic Oxygenation Events In The Anoxic Ediacaran Ocean. *Geobiology*, 14, 457–468.
- Sahoo, S. K., Planavsky, N. J., Kendall, B., et al., 2012. Ocean Oxygenation in the Wake of the Marinoan Glaciation. *Nature*, 489(7417): 546–549
- Scott, C., Lyons, T. W., Bekker, A., et al., 2008. Tracing the Stepwise Oxygenation of the Proterozoic Ocean. *Nature*, 452(7186): 456–459
- Tribouillard, N., Algeo, T. J., Baudin, F., et al., 2012. Analysis of Marine Environmental Conditions Based On Molybdenum-Uranium Covariation—Applications to Mesozoic Paleocyanography. *Chemical Geology*, 324–325: 46–58
- Tribouillard, N., Algeo, T. J., Lyons, T., et al., 2006. Trace Metals as Paleoredox and Paleoproductivity Proxies: An Update. *Chemical Geology*, 232(1–2): 12–32
- Vernhet, E., Reijmer, J. J. G., 2010. Sedimentary Evolution of The Ediacaran Yangtze Platform Shelf (Hubei And Hunan Provinces, Central China). *Sedimentary Geology*, 225(3–4): 99–115

- Wignall, P. B., Twitchett, R. J., 1996. Oceanic Anoxia and the End Permian Mass Extinction. *Science*, 272(5265): 1155–1158
- Xiao, S., Muscente, A., Chen, L., et al., 2014. The Weng'an Biota and the Ediacaran Radiation of Multicellular Eukaryotes. *National Science Review*, 1(4): 498–520
- Xiao, S., Yuan, X. L., Steiner, M., et al., 2002. Macroscopic Carbonaceous Compressions in a Terminal Proterozoic Shale: A Systematic Reassessment of the Miaohu Biota, South China. *Journal Of Paleontology*, 76(2): 347–376
- Xiao, S., Zhang, Y., Knoll, A., 1998. Three-Dimensional Preservation of Algae and Animal Embryos in a Neoproterozoic Phosphorite. *Nature*, 391(6667): 553–558
- Xin, H., Jiang, S.Y., Yang, J.H., et al., 2016. Rare Earth Element Geochemistry of Phosphatic Rocks in Neoproterozoic Ediacaran Doushantuo Formation in Hushan Section from the Yangtze Gorges Area, South China. *Journal of Earth Science*, 27(2): 204–210.
- Yin, L., Zhu, M., Knoll, A. H., et al., 2007. Doushantuo Embryos Preserved inside Diapause Egg Cysts. *Nature*, 446(7136): 661–663
- Zhai, L., Wu, C., Ye, Y., et al., 2016. Marine Redox Variations during the Ediacaran/Cambrian Transition on the Yangtze Platform, South China. *Geological Journal*. doi: 10.1002/Gj
- Zhu, M., Lu, M., Zhang, J., et al., 2013. Carbon Isotope Chemostratigraphy and Sedimentary Facies Evolution of the Ediacaran Doushantuo Formation in Western Hubei, South China. *Precambrian Research*, 225: 7–28
- Zhu, M., Zhang, J., Yang, A., 2007. Integrated Ediacaran (Sinian) Chronostratigraphy of South China. *Palaeogeography, Palaeoclimatology, Palaeoecology*, 254(1–2): 7–61
- Zheng, Y., Anderson, R. F., Van Geen, A., et al., 2000. Authigenic Molybdenum Formation in Marine Sediments: A Link to Pore Water Sulfide in the Santa Barbara Basin. *Geochimica et Cosmochimica Acta*, 64(24): 4165–4178
- Zhou, C., Jiang, S.Y., 2009. Palaeoceanographic Redox Environments for the Lower Cambrian Hetang Formation in South China: Evidence From Pyrite Framboids, Redox sensitive trace elements, and sponge biota Occurrence. *Palaeogeography, Palaeoclimatology, Palaeoecology*, 271(3–4): 279–286
- Zhou, C. M., Xie, G. W., Mcfadden, K., et al., 2007. The Diversification and Extinction of Doushantuo-Pertatataka Acritarchs in South China: Causes and Biostratigraphic Significance. *Geological Journal*, 42(3–4): 229–262
- Zhu, B., Becker, H., Jiang, S. Y., et al., 2013. Re-Os Geochronology of Black Shales from the Neoproterozoic Doushantuo Formation, Yangtze Platform, South China. *Precambrian Research*, 225: 67–76
- Zhu, M. Y., Zhang, J. M., Steiner, M., et al., 2003. Sinian-Cambrian Stratigraphic Framework for Shallow-to Deep-Water Environments of the Yangtze Platform: An Integrated Approach. *Progress in Natural Science*, 13(12): 951–960